

JOURNAL OF ENVIRONMENTAL HYDROLOGY

The Electronic Journal of the International Association for Environmental Hydrology

On the World Wide Web at <http://www.hydroweb.com>

VOLUME 17

2009



ENVIRONMENTAL TRACERS AS INDICATORS OF WATER FLUXES THROUGH THE UNSATURATED ZONE IN SEMIARID REGIONS: THE CASE OF GAFSA PLAIN (SOUTHERN TUNISIA)

Messaouda Yermani¹

Najiba Chkir²

Kamel Zouari³

Jean Luc Michelot⁴

Lahmadi Mounni⁵

¹Departement de Biologie-Géologie, Institut Préparatoire aux Etudes d'Ingénieurs de Bizerte, Tunisia

²Laboratory of Radio-Analysis and Environment, Department of Geography, Faculty of Arts and Humanities, Sfax, Tunisia

³Laboratory of Radio-Analysis and Environment, Department of Geology, National School of Engineers, Sfax, Tunisia

⁴UMR CNRS-UPS "IDES", Université Paris-Sud, Orsay, France

⁵Commissariat au Développement Agricole de Tozeur, Ministry of Agriculture and Water Resources, Tunisia

Isotopic and chloride investigations have been conducted to estimate local hydrologic processes taking place in the semiarid Gafsa Plain (Southern Tunisia). A sandy soil core has been sampled at one site where the water table is at about 6 m depth and where water level fluctuations indicate a direct recharge of the shallow aquifer. Oxygen 18 and chloride data have been interpreted using the model of Barnes and Allison to suggest that evaporation rates from groundwater average around 11 mm/y. The rates from the shallow aquifer level to the soil surface range from 7 to 22 mm/y. The model parameters highlight that evaporation mechanisms are increasingly dominated by vapor phase transfers as the thickness of the layer through which water evaporates increases. The recharge rates by direct rainfall infiltration have been estimated by chloride mass balance method to range from 3 to 5 mm/y, with a mean value of 3.9 mm/y. This represents about 2.4% of local rainfall (164 mm/year). The long residence time of 77.8 years shown by the 6m depth chloride profile indicates slow recharge processes.

INTRODUCTION

In arid and semiarid areas, groundwater is often the single resource available to supply human needs, thus a reliable knowledge of the water balance is necessary to ensure a sustainable management of water resources. Nowadays, the assessment of evaporation rate remains difficult to estimate due to several causes including costly direct measurements. Even if the upper first few meters of the soil profile are the hydrologically most active in these regions due to the strong influence of environmental changes such as temperature and precipitation on soil water and solutes, basic methods founded on climatic and/or hydrodynamic parameters are strongly limited by very low ranges of hydrological fluxes. Theoretical and experimental studies (Zimmermann et al. 1967; Barnes and Allison 1983; Sonntag et al., 1985) showed that the isotopic composition of groundwater in arid areas can be interpreted in terms of evaporation rates. Induced methodologies were extended for the study of unsaturated zones (Allison and Hughes, 1983; Fontes et al., 1986). In addition, chloride is hydrologically very mobile and chemically very inert, and therefore can be considered as a nearly ideal natural tracer for the study of soil water movement in the liquid phase, and for the estimation of long-term average infiltration rates (Gaye and Edmunds, 1996; Cook et al. 1992; Liu et al. 1995). The efficiency of chloride profile based methods is also corroborated by stable isotope profile interpretations (Fontes et al., 1986).

In the Gafsa Plain, southern Tunisia, previous studies (IGIP, 1998) have evaluated infiltration rates using rainfall-runoff relationships for different ranges of permeability. These studies have estimated an infiltration rate around 2% of precipitation for low permeability unsaturated sediments (10^{-7} m/s) and around 5% for high permeability ones (10^{-3} m/s). Another approach based on spring discharge suggested an infiltration rate ranging between 15 and 18% of precipitation (IGIP, 1998). However, evaporation rates from the aquifer have never been quantified.

The objective of this study is to apply the environmental tracers ^{18}O and Cl to an investigation of infiltration and evaporation rates in the unsaturated zone in the Gafsa Plain.

SITE DESCRIPTION

The northern Gafsa Plain is situated in central Tunisia (Figure 1). It extends over an area of 3750 km² north of the town of Gafsa between latitudes 38°22'N and 38°61'N and longitudes 6°81'E and 7°6'E. This plain is delimited from north to northeast successively by Jebel Sidi Aïch, Souinia, Majoura and ElGoussa, in the east by the Orbata and Bou Hedma anticlines, in the south by jebel Orbata and the Gafsa fault, in the southwest by jebels Ben Younès and Bou Ramli, and in northwest by the plate of Majen Bel Abbès.

The plain of Gafsa is located in central Tunisia where both occidental Mediterranean and Saharan systems coming respectively from the north and from the south influence climate. The plain is characterized by semiarid conditions with low rainfall averaging 164 mm/year distributed on 13 to 50 days and a high mean annual temperature around 19°C. The plain is marked by regular topography with a main slope towards the south. Altitudes decrease from 650 m in the area of Majen Bel Abbès to less than 300 m around Gafsa. The hydrographic network is endoreïc. The western part of the plain is crossed by wadi el Kébir and wadi Sidi Aïch while in the eastern part, wadis originating from the surrounding jebels reach wadi el Melah but only during rare flooding periods.

The Ouled M'Hamed survey zone is located in the central part of the northern plain of Gafsa. Topography is rather flat, the land is generally barren, with few olive and cactus plants. In this area,

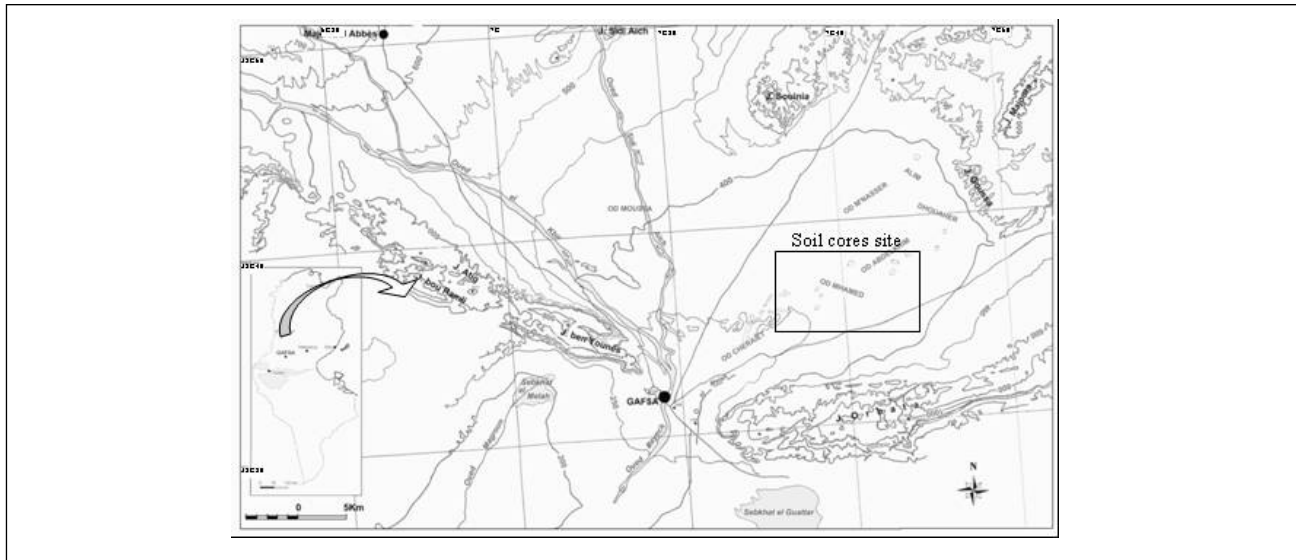


Figure 1. Geographical location of the Plain of Gafsa.

groundwater resources have been highly exploited for a long time. This is due the fact that the water level is close to the surface with a depth that does not exceed 10 m allowing direct and easy access for human uses.

The subsurface lithology presents important lateral and vertical variations. Geological formations in core S1 (Figure 2) are mainly sandy. Two kilometers south of this core, core S2 of 7.5 m depth has several strata of clays and gypsum whose frequency and thickness increase with depth. The core sites are exposed to a typical Mediterranean climate with two contrasted seasons: a dry hot summer extending from May to October during which temperatures are higher than the annual mean and can reach extreme values as 45°C. During this season, rainfall is less than 20% of the annual mean and is mostly nonexistent. The second season is relatively wet and warm, temperatures are less than the annual mean and can reach extreme values as 6°C while rainfall is about 80% of the annual average.

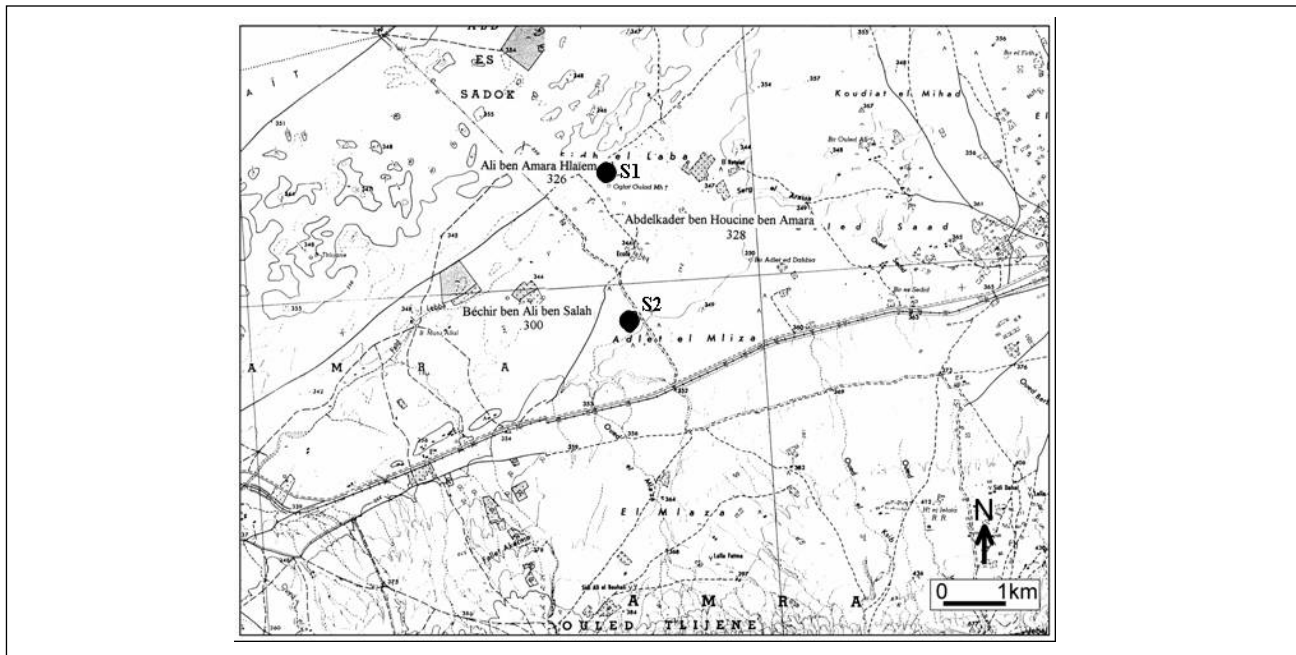


Figure 2. Location of the core S1 for the study of the unsaturated zone.

Three wells located nearest the core sites have been chosen from the shallow aquifer monitoring network of northern Gafsa in order to follow water level fluctuations in response to rainfall (Figure 3).

In the Oulet M'Hamed zone, where wells DRE163 and DRE272 are located, clayey and gypsum intercalations reduce the aquifer recharge by retaining water and favoring lateral subsurface movement when saturated. In the case of well DRE621 rainfall crossing sandy geological layers moves by a piston flow mechanism rain water previously stored in the unsaturated zone, which then reaches the aquifer and causes a rise of the water table. This zone is considered appropriate for the location of the S1 core to study infiltration and the evaporation through the unsaturated zone.

Hydrochemical analyses (standard protocols) have been carried out on groundwater sampled around the core site in order to characterize the shallow aquifer under the unsaturated zone. Results have been supplemented by data from the water resources office of Gafsa (CRDA, 2000). Groundwaters are highly mineralized with a mean salinity ranging around 5 g/l and a maximum value over 15 g/l. This has been explained by high evaporation (Farhat and Moumni, 1989). On the other hand, the lithology of the subsoil associated with a very weak hydraulic gradient (0.5 %) can facilitate the concentration of dissolved salts in water. The chemical facies is generally mixed sulfate.

UNSATURATED ZONE STUDY

Materials and methods

The flux of water in the unsaturated zone has been estimated for a core from a mechanical auger at site S1 in the Ouled M'Hamed zone. The core crosses the entire thickness of the unsaturated zone which is made up of fine to coarse sands (Figure 4a). The water table of the shallow aquifer was located at 4.85 m. The soil profile was determined with a sampling interval of 5-10 cm to a depth of 5.45 m. Several different analyses have been carried out in the laboratory:

- The relative importance of the liquid phase in the soil is measured by the volumetric water content (θ) and by the mass water content (w), that are directly related by the soil apparent density (d) measured by a mercury pycnometer to a value of 1.3 g/cm³ (Musy and Soutter, 1991).

- The chemical composition the soil water has been obtained by the lixiviation of the soil sample. A volume of distilled water (V_{lix}) is added to a mass of soil (M_s) and then submitted to mechanical continuous shaking until the stabilization of the conductivity. The lixiviat is filtered through a 0.45 μ m filter and then analyzed for different chemical elements. For each analyzed element, the concentration of the soil water (C_i) is related to the concentration of the lixiviat (C_{lix}) given the mass water content of the soil (w) as in Equation 1.

$$C_i = \frac{V_{lix} \cdot C_{lix}}{w \cdot M_s} \quad (1)$$

- For the isotopic contents (¹⁸O and deuterium), soil water (100 g) is extracted by distillation under vacuum conditions at 50°C during 8 h, then water is condensed and trapped in tubes under low temperature (-188°C) for isotope analysis (Gouvea Da Silva Rosa, 1980).

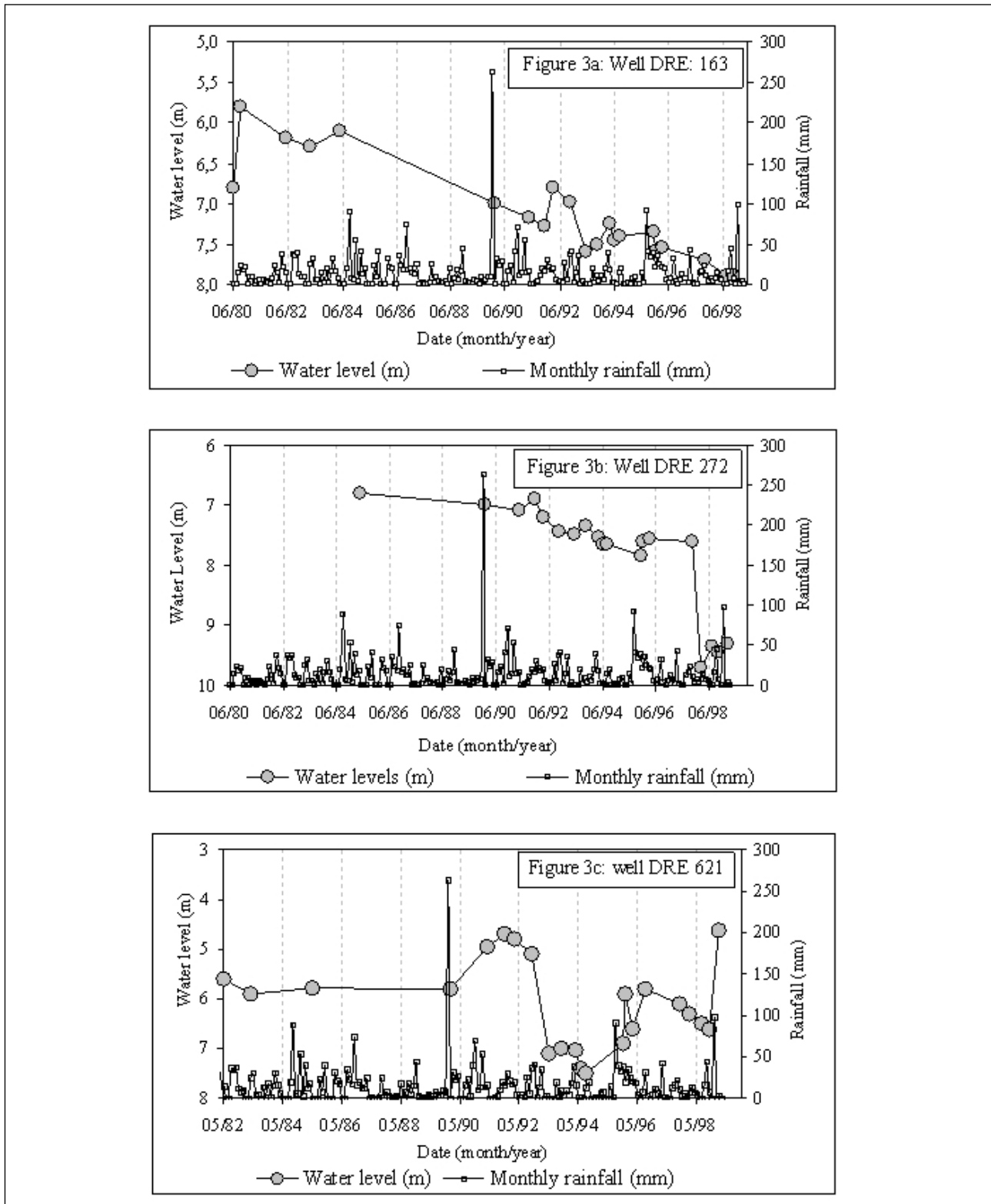


Figure 3. Water levels fluctuations and rainfall for three shallow aquifer wells.

Analytical data

The volumetric water content of the first 20 cm layer averages around 5% and remains quite constant up to a depth of 365 cm (Figure 4b). Beyond this depth, the volumetric water content increases up to its maximum value (22%) at the 465 cm limit indicating the influence of the capillary fringe ascending water movement from the saturated zone.

The stable isotope content profile shows the characteristic trend of an evaporation profile from the surface to the shallow aquifer with a succession of picks (Figure 4c). Assuming that the water movement in the unsaturated zone is of piston flow type, negative picks correspond to rainy episodes separated by positive picks from dry periods (Grünberger, 1989). Consequently, the profile has been divided into five evaporation phases (A, B, C, D, E) with the base of each one coinciding with a negative pick. The evaporation phenomenon is well identified on the oxygen 18 vs deuterium diagram where all points plot under the GMWL along a line with a slope of 1.7 that indicates a strong evaporation effect (Figure 5). This evaporation line, plotted for the whole water soil profile is influenced by points of the A phase, whose evaporation line slope is around 1.06. Indeed, the evaporation effect is higher closer to the surface. The low slope (1.06) indicates a kinetic evaporation phenomenon close to the one induced by a pure molecular diffusion of the water vapor (1.026 slope) such as that observed in several other studies for subsurface layers (Gouvea Da Silva Rosa, 1980; Allison and Hughes, 1983).

According to Barnes and Allison (1983), the slope for water evaporating from dry soils ranges generally around 3. However, a slope of 1.7 is too low to be explained by the contribution of kinetic evaporation to the total enrichment (a minimum slope of 2.7). Fontes et al. (1986) have explained this phenomenon by a mixing of waters from previous infiltration events both above and below the evaporation front.

The chloride profile for the soil water of the core is also characteristic. It can be seen that the first chemical evaporation front indicated by the pick situated nearest the surface does not coincide with the isotopic evaporation front.

PRINCIPLE OF THE MODEL

Isotopic model

A soil containing a shallow aquifer with an isotopic content (δ_{res}) and a certain ion concentration (C_{res}), when submitted to an atmosphere with a relative humidity (h) and with a water vapor isotopic content (δ_{at}), if not recharged by precipitation, will dry and the mechanism of water transport will

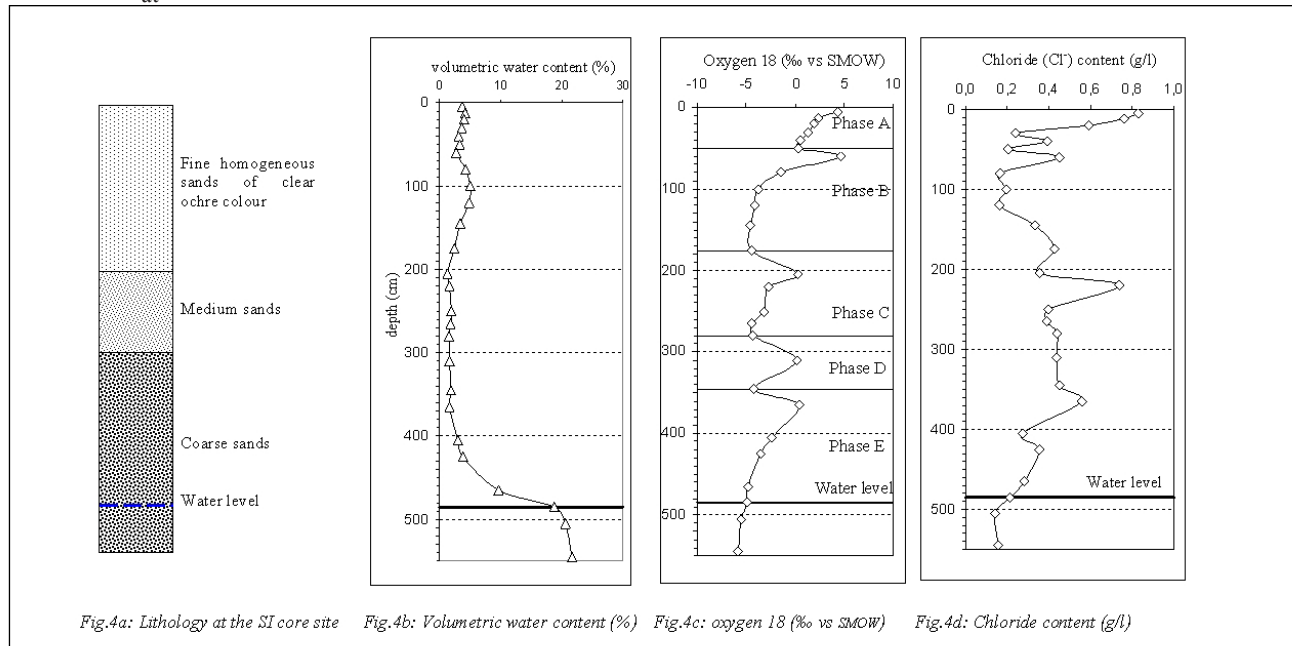


Figure 4. Characteristics of soil core profile in Ouled M'Hamed site (S1) function of depth.

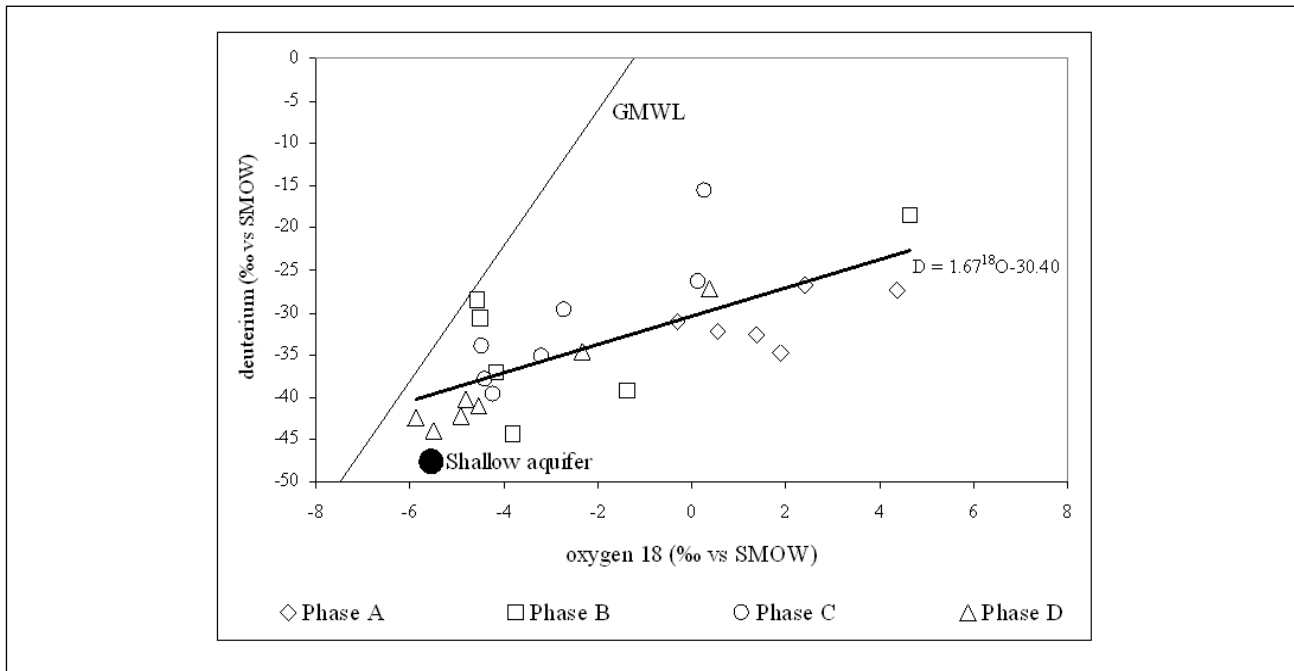


Figure 5. Stable isotopes diagram for soil water of the core S1 compared to the shallow aquifer isotopic signal.

set up under its two liquid and solid forms. After a certain time t , an equilibrium regime during which the humidity fluxes are constant will be established. Stable isotope (^{18}O and D) profiles will take an exponential shape from the surface of the aquifer (Doering et al., 1963). A characteristic isotopic profile for a soil submitted to an evaporative regime under flow equilibrium (Barnes and Allison, 1983) shows two parts:

- A zone where the transfer is in the vapor phase and the isotopic gradient is positive. The profile varies from a minimum value at the surface ($\delta_{\text{at}} + \epsilon_{(1-v)}$) to a maximum value (δ_{ef}) located at the evaporation front with a Z_{ef} depth. It is a diffusion zone where both evaporated and atmospheric vapor fluxes are mixed;

- A zone of a composite transfer of liquid and vapor phases where isotopic contents decrease from δ_{ef} to δ_{res} .

If a temperature variation is considered, isotopic profiles will reach lower values than δ_{res} and the evaporation front will be deeper with a more depleted isotopic content. As the variation of temperature in soil is weak for the present case study, the model is only presented for isothermal conditions. Under arid conditions, long periods between infiltration events allow soil profiles to equilibrate in steady state conditions. The evaporation rate is constant through both zones defining the isotopic profile (Taupin, 1995). In the composite transfer zone, the profile is described as follows (Equation 2):

$$\delta_z = (\delta_{\text{ef}} - \delta_{\text{res}}) \exp\left(\frac{-f(z)}{Z_L}\right) + \delta_{\text{res}} \quad (2)$$

where δ_z is the isotopic content (‰ vs SMOW) at a depth z , and Z_L is the mean diffusion depth of the isotope into the soil in liquid phase (m). Two cases have to be considered for the weighting function $f(z)$.

If the vapor flux is significant $f(z)$ is given by Equation 3:

$$f(z) = \bar{\theta} \int_{z_{ef}}^z \left(\theta + \left[\frac{N_{sat} D_{atm} (n - \theta)}{\rho_w D_{liq}} \right] \right)^{-1} dz \quad (3)$$

where N_{sat} is the saturated water vapor content of the soil (Kg/m^3) depending on the temperature, D_{atm} and D_{liq} are the diffusivity of the isotope respectively in the air and in water depending on temperature (De Vries and Kruger, 1967); n is the porosity of the soil; θ is the volumetric water content; and ρ_w is the density of liquid water (Kg.m^{-3}).

- If the liquid phase is dominant then $f(z)$ is given by Equation 4:

$$f(z) = \int_{z_{ef}}^z \sigma \cdot dz \quad (4)$$

where σ is the excess of the isotope diffusion rate in vapor phase as given by recent measurements to be 1.032 (Cappa et al., 2003) rather than 1.028 (Merlivat, 1978).

The ratio between the liquid (Q_L) and the vapor fluxes (Q_V) (Equation 5) allows identifying which case has to be retained:

$$\frac{Q_v}{Q_l} \approx \frac{Z_v}{Z_L} \approx \frac{N_{sat} \cdot D_{atm} \cdot \overline{n - \theta}}{\rho_w \cdot D_{liq} \cdot \bar{\theta}} \quad (5)$$

where Z_V is the mean diffusion depth (m) of the isotope into the soil in vapor phase.

The model is defined by the $1/Z_L$ parameter obtained by a linear least squares optimization of the weighting function $f(z)$ on $\ln \left[\frac{(\delta_z - \delta_{res})}{(\delta_{ef} - \delta_{res})} \right]$. The δ_{res} and δ_{ef} values are taken from the isotope content profile and weakly modified to improve the fit between measured and calculated isotope content values. The evaporation vertical flux (E) is given by the following equation (Equation 6):

$$E = \frac{\bar{\theta} * \tau * D_{liq}}{Z_L} \quad (6)$$

where τ is the tortuosity of the soil. As the soil texture is principally composed of medium and coarse sand, the tortuosity value was estimated between 0.6 and 0.67 (Penman, 1940).

Chloride model

The purpose here is to estimate the groundwater recharge using the chloride profiling method. Environmental chloride is deposited on land by atmospheric deposition processes (rainfall and dry fallout). If the chloride present in the unsaturated zone has atmospheric deposition as its source and if there is no other source or sink in the unsaturated zone for the chloride ions, then under steady state conditions assuming piston flow, it is possible to obtain a chloride mass balance for the chloride flux entering and leaving the root zone (Taupin, 1995; Scanlon, 1991; Gaye and Edmunds, 1996). Given these conditions, for each layer of soil, the chloride balance is given by the equilibrium between the mean concentration of chloride in soil water (C_p) and the mean recharge (R), or between the mean chloride concentration of rainfall (C_p) and the mean annual

rainfall (P) as expressed in Equation 7 (Edmunds and Walton, 1980):

$$R = \frac{P \cdot C_p}{C_s} \quad (7)$$

Assuming that the soil profile has come to a chemical equilibrium, the residence time (t) of the quantity of chloride ions stored in a certain depth of soil (H) is expressed as follows (Equation 8) (Cook et al., 1992; Edmunds et al., 1999).

$$t = \int_0^H \frac{C_s \cdot \theta}{C_p \cdot P} \cdot dz \quad (8)$$

The recharge rate of each evaporation phase is the average of recharge rates calculated for each soil layer of the phase weighted by the corresponding residence time.

RESULTS AND DISCUSSION

The evaporation model has been applied for each evaporative phase indicated by the core profiles (Phase A, Phase B, Phase C, Phase D, Phase E) according to the oxygen 18 content profile (Table 1). The temperature has been considered constant for all depth, equal to the annual average temperature (T=19°C). The values of the different variables depending on temperature are $N_{\text{sat}}=15.61 \times 10^{-3} \text{ Kg/m}^3$, $D_{\text{atm}}=0.241 \times 10^{-4} \text{ m}^2/\text{s}$ and $D_{\text{liq}}=1.78 \times 10^{-9} \text{ m}^2/\text{s}$.

The Z_v/Z_L ratio (Equation 5) calculated for each phase shows an increase from 1.35 in the subsurface soil layer (Phase A, 0-50 cm) up to 3.09 at the depth of Phase D (280-345 cm) indicating that the importance of vapor transfer increases as the evaporation front is deeper in the soil. The Phase E (345-545 cm) takes place in the zone influenced by the capillary ascending water movement as shown by the water content profile. This could explain the predominance of liquid transfer ($Z_v/Z_L=0.29$). Consequently, the composite transfer model has been applied (Equation 3) for all phases except for the interval E for which the liquid transfer model has been applied (Equation 4). All functions reveal good linearity with r^2 ranging from 0.85 to 1 (Figure 6) and a good agreement is observed between calculated and measured oxygen 18 content (Figure 7). Except for the subsurface layer, $d_{\text{res}}^{18}\text{O}$ values are also quite constant ranging between -5 and -6.5 ‰ vs SMOW close to the signature of the shallow aquifer (Yermani, 2000). The $d_{\text{res}}^{18}\text{O}$ allowing the best fit for the subsurface evaporative phase (A) is more enriched (0‰ vs SMOW) probably due to the fact that the soil water sampled at the bottom of this phase profile is a mixture between originating water (shallow aquifer) and enriched water (evaporation effect on infiltrated water).

The ZL parameter (Equation 2) has been extracted for each evaporative phase and reported for the estimation of the evaporation rates (Equation 6) depending on $t = 0.6$ or 0.67 (Table 2). Mean evaporation rates vary from 22 to 7 mm/year from the near surface phase to the deeper one at 545 cm depth. A linear relationship is observed between the inverse of the evaporation rate and the thickness of the soil above the evaporation phase (Figure 8) as previously observed by Allison et al. (1983). If we ignore the two extreme values influenced by the surface for the top of the core and by the shallow water table for the bottom, an annual mean evaporation rate of 11 mm/year can be estimated using a steady-state model. The potential regional evapotranspiration rate is 1533-1638 mm/y. (Yermani, 2000). This suggests that less than 1% of water losses can be provided by the aquifer through the unsaturated zone.

Table 1. Calibration of the isotopic model for the profile of the core S1.

Evaporation Phase	Depth (cm)	$\delta^{18}O$ measured	θ	$f(z)$	$Ln \left(\frac{\delta_z - \delta_{res}}{\delta_{ef} - \delta_{res}} \right)$	$\delta^{18}O$ simulated	Isotopic model
A	5	4.37	0.048	0.021	-0.317	4.55	$Ln \left(\frac{\delta_z - \delta_{res}}{\delta_{ef} - \delta_{res}} \right) = -13013 \times f(z) - 0.09$ $r^2 = 0.978; \delta_{res} = 0$ and $\delta_{ef} = 6$ (‰ vs SMOW).
	12	2.4	0.054	0.050	-0.916	3.15	
	20	1.88	0.052	0.082	-1.160	2.05	
	30	1.37	0.047	0.125	-1.477	1.18	
	40	0.56	0.040	0.170	-2.372	0.66	
	50	0.32	0.042	0.214	-2.931	0.37	
B	60	4.64	0.035	0.048	-0.442	4.52	$Ln \left(\frac{\delta_z - \delta_{res}}{\delta_{ef} - \delta_{res}} \right) = -9.481 \times f(z) -$ $r^2 = 0.975; \delta_{res} = -5$ and $\delta_{ef} = 10$ (‰ vs SMOW).
	80	-1.39	0.055	0.131	-1.424	-0.68	
	100	-3.8	0.065	0.209	-2.526	-2.93	
	120	-4.14	0.062	0.288	-2.859	-4.02	
	145	-4.56	0.044	0.400	-3.529	-4.66	
	175	-4.49	0.031	0.549	-5.521	-4.92	
C	205	0.26	0.016	0.073	-1.048	-0.23	$Ln \left(\frac{\delta_z - \delta_{res}}{\delta_{ef} - \delta_{res}} \right) = -14355 \times f(z) - 0.14$ $r^2 = 0.888; \delta_{res} = -5$ and $\delta_{ef} = 10$ (‰ vs SMOW).
	220	-2.72	0.021	0.104	-1.884	-1.71	
	250	-3.2	0.025	0.163	-2.120	-3.50	
	265	-4.46	0.024	0.193	-3.324	-4.05	
	280	-4.39	0.020	0.224	-3.202	-4.46	
D	310	0.15	0.021	0.075	-1.074	0.10	$Ln \left(\frac{\delta_z - \delta_{res}}{\delta_{ef} - \delta_{res}} \right) = -14513 \times f(z) + 0.00$ $r^2 = 1; \delta_{res} = -6$ and $\delta_{ef} = 12$ (‰ vs SMOW).
	345	-4.21	0.024	0.160	-2.308	-4.23	
E	365	0.39	0.021	0.206	-0.321	0.77	$Ln \left(\frac{\delta_z - \delta_{res}}{\delta_{ef} - \delta_{res}} \right) = -1.296 \times f(z) - 0.05$ $r^2 = 0.993; \delta_{res} = -6.5$ and $\delta_{ef} = 3$ (‰ vs SMOW).
	405	-2.33	0.038	0.619	-0.823	-2.24	
	425	-3.54	0.049	0.826	-1.166	-3.24	
	465	-4.82	0.126	1.238	-1.732	-4.59	
	485	-4.92	0.243	1.445	-1.794	-5.04	
	505	-5.5	0.282	1.651	-2.251	-5.38	
	545	-5.88	0.268	2.064	-2.729	-5.85	

Mean chloride concentration (C_p) of rainfall is taken equal to 8 mg/l by comparison to the meteorological station of Sfax (IAEA/WMO, 2004) with a mean annual precipitation recorded at the nearest meteorological station of Gafsa SM equal to 164 mm (Yermani, 2000). The recharge rate has been estimated for each sampled interval of the core S1 (Table 3). The recharge rate of each evaporative phase as indicated by isotopic and chloride profiles is the average of recharge rates calculated (Equation 8) for each soil layer of the phase, weighted by the corresponding residence time. If the deeper phase where the recharge rate is probably over estimated due to the capillarity effect, the mean recharge rate along the soil core profile ranges between 3 and 5 mm/year.

Transit time of percolation water along the core S1 (Table 3) indicates that the total profile has taken place during 77.8 years. This residence time refers to a percolation velocity of $V=0.06m/year$, and with a mean water content in the unsaturated zone of 5% to a recharge of $R=3mm/year$ ($R=nV$). Considering that the sampling campaign was carried out in March 1997, probable dates of infiltration events separating the evaporation phases have been extracted from the precipitation time-series. It is noticeable that each infiltration event corresponds to local extreme flooding events such as those of 1989 or 1969.

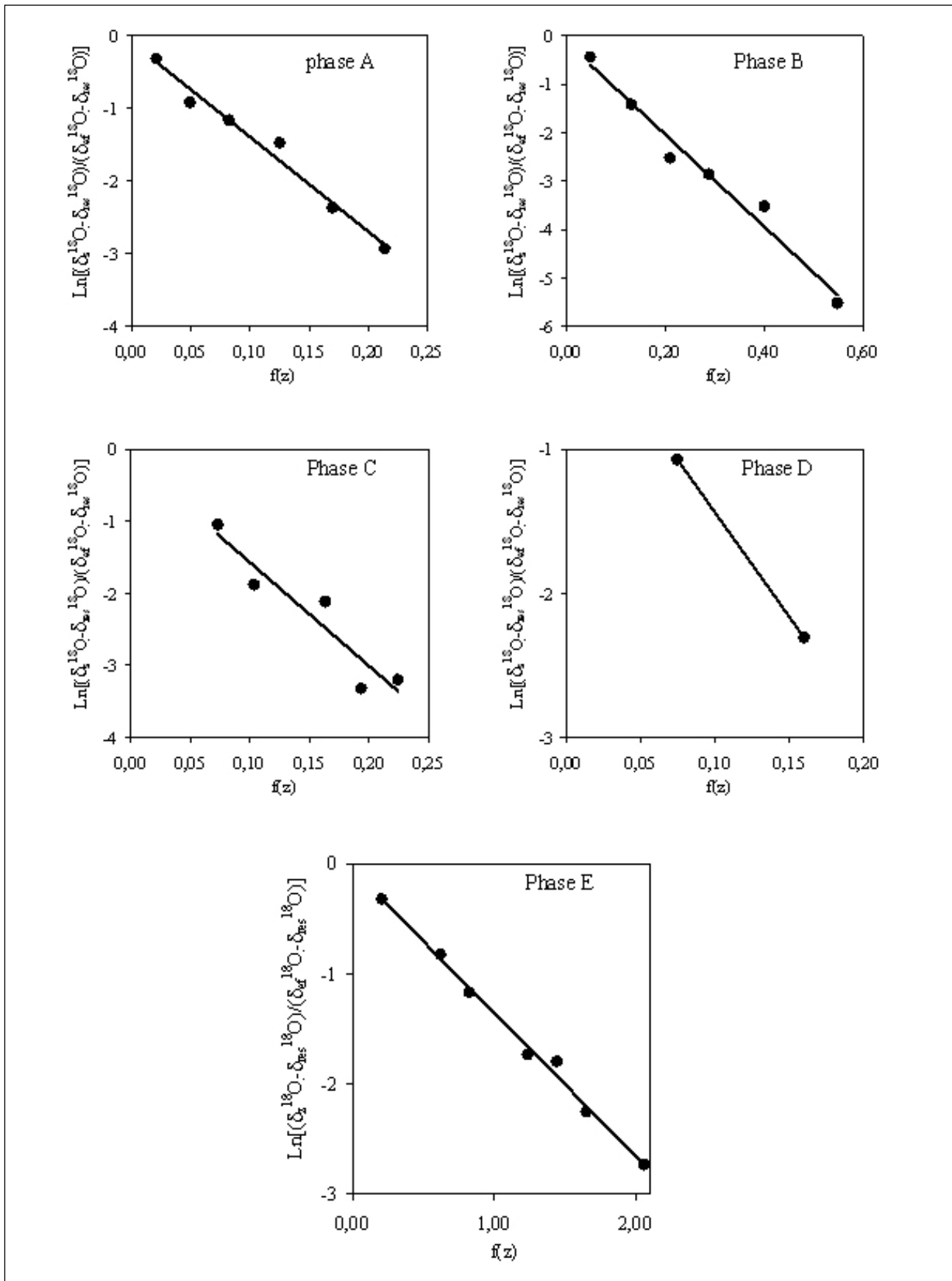


Figure 6. Isotopic model for the S1 core profile :relationship between $f(z)$ and $\text{Ln}[(\delta_z^{18}\text{O} - \delta_{\text{res}}^{18}\text{O}) / (\delta_{\text{ef}}^{18}\text{O} - \delta_{\text{res}}^{18}\text{O})]$.

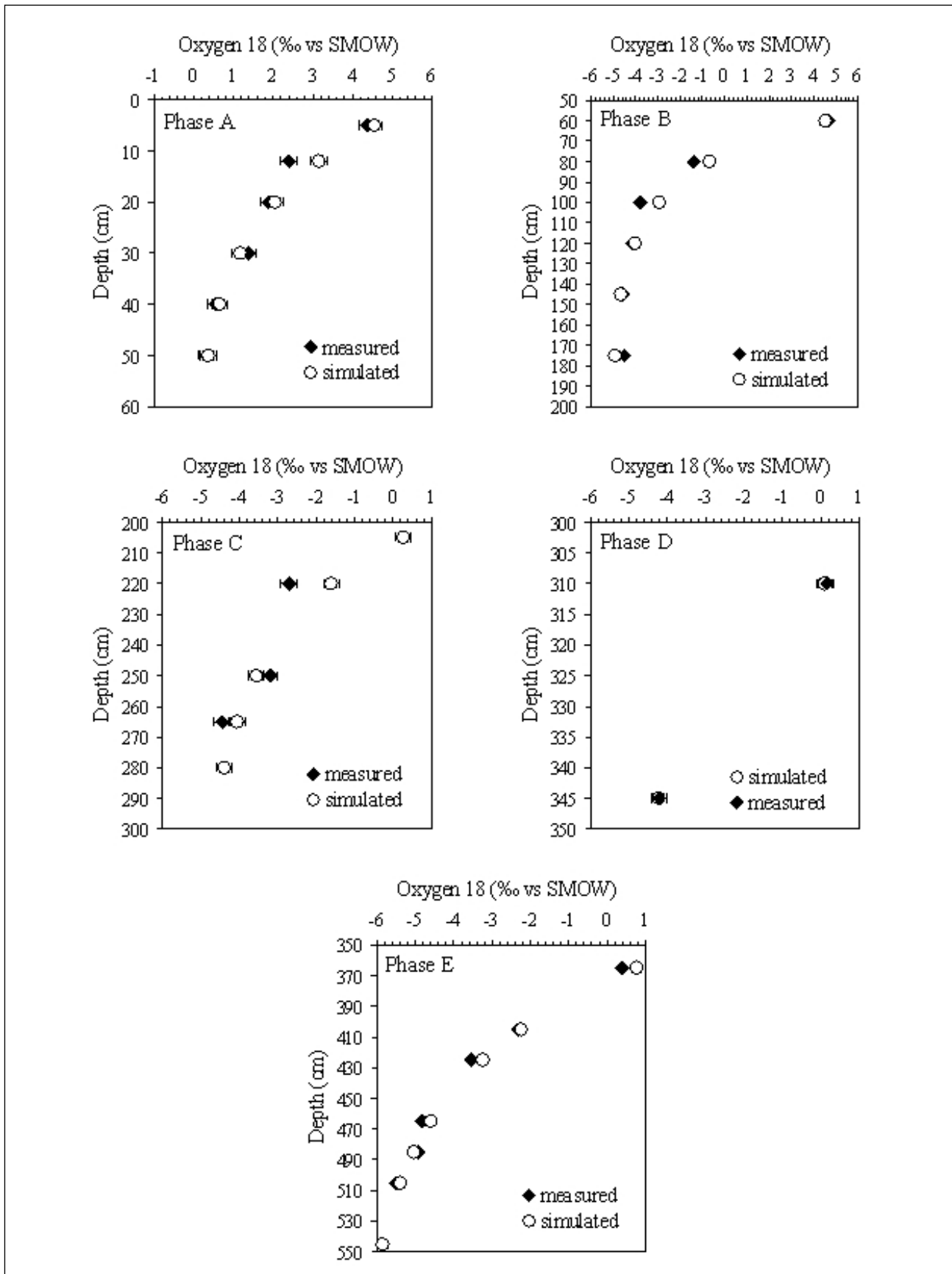


Figure 7. Isotopic model for the S1 core profile: measured and simulated oxygen 18 content (‰ vs SMOW).

Table 2. Evaporation rates.

Phase	Thickness of the soil above the phase (cm)	Evaporation rate (mm/year)		Mean Evaporation rate (mm/year)
		$\delta = 0.6$	$\delta = 0.67$	
A	50	20,7	23,2	22,0
B	175	15,6	17,4	16,5
C	280	10,2	11,4	10,8
D	345	11,0	12,3	11,7
E	200	6,4	7,2	6,8

The comparison of recharge rate to cumulative precipitation between infiltration events gives an estimation of infiltration rate for each phase. Except for the deeper soil layer (365-545 cm) where the capillarity effect has increased the soil water content, infiltration ranges between 2 and 3% of annual precipitation.

CONCLUSIONS

In arid zones, long dry periods allow the isotope profile to reach an equilibrium state between vertical water and vapor fluxes in the unsaturated zone. However, important infiltration events can interrupt this process by the mixture between enriched evaporated water and infiltrated rainwater. Consequently, the isotope profile is made up of successive evaporation phases during which typical isotope variation can be recognized. This work has been carried out on a soil core sampled in an arid zone with a near surface shallow aquifer. The isotopic model adequately describes the five evaporation phases recognized on the oxygen 18 profile. The ratios between the liquid and the vapor fluxes estimated for each of these phases indicate that the water transfer during evaporation mainly takes place in composite liquid-vapor phase. However, the vapor phase maximum in the near surface soil layer decreases with depth. In the study case, a capillary ascending movement of water from the shallow aquifer has influenced the isotopic profile of the deeper evaporation phase allowing the liquid phase transfer to become dominant. The calibration of the model shows that the originating water has the same isotopic signal as the shallow aquifer confirming that the main origin of evaporated water through the unsaturated zone comes from the aquifer rather than the infiltrated rainwater. The mean evaporation rate through the unsaturated zone increases as the surface becomes closer. A mean evaporation rate of 11 mm/year is retained with a minimum of

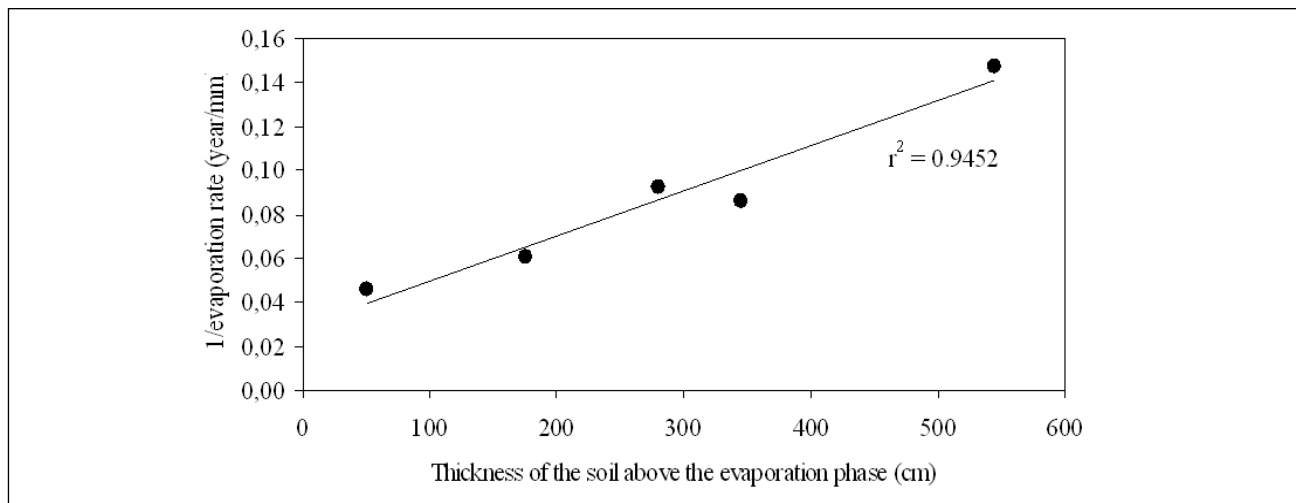


Figure 8. Linear relationship between the inverse of the evaporation rate and the thickness of the soil

Table 3. Infiltration parameters by chloride balance in the core S1.

Depth (cm)	θ (%)	Cumul (mm)	Cl ⁻ (mg/l)	Σ Cl ⁻ (g/m ³)	Cl ⁻ age (year)	Σ age (year)	Recharge (mm/y.)	Mean recharge (mm/y.)
0	5	4.79	2.39	830.2	1.99	1.51	1.51	1.6
5	12	5.43	6.20	761.2	4.88	2.21	3.72	1.7
12	20	5.20	10.36	590.3	7.34	1.87	5.59	2.2
20	30	4.70	15.06	239.9	8.47	0.86	6.45	5.5
30	40	4.04	19.10	392.4	10.05	1.21	7.66	3.3
40	50	4.24	23.34	202.5	10.91	0.65	8.31	6.5
50	60	3.50	26.84	450.8	12.49	1.20	9.52	2.9
60	80	5.47	37.78	164.4	14.29	1.37	10.89	8.0
80	100	6.53	50.84	195.8	16.84	1.95	12.84	6.7
100	120	6.24	63.32	160.2	18.84	1.52	14.36	8.2
120	145	4.39	74.30	331.9	22.49	2.78	17.14	3.9
145	175	3.11	83.64	426.4	26.47	3.03	20.18	3.1
175	205	1.65	88.59	355.4	28.23	1.34	21.52	3.7
205	220	2.07	91.69	738.2	30.52	1.75	23.26	1.8
220	250	2.47	99.10	396.6	33.46	2.24	25.50	3.3
250	265	2.35	102.64	387.8	34.83	1.04	26.55	3.4
265	280	2.03	105.68	440.4	36.17	1.02	27.57	3.0
280	310	2.12	112.04	437.2	38.95	2.12	29.69	3.0
310	345	2.39	120.40	450.7	42.72	2.87	32.56	2.9
345	365	2.09	124.59	557.7	45.05	1.78	34.34	2.3
365	405	3.84	139.94	273.5	49.25	3.20	37.54	4.8
405	425	4.94	149.82	352.7	52.74	2.65	40.20	3.7
425	465	12.57	200.10	281.8	66.91	10.80	51.00	4.7
465	485	24.34	248.79	213.6	77.31	7.93	58.92	6.1
485	505	28.16	305.10	142.4	85.32	6.11	65.03	9.2
505	545	26.76	412.12	156.0	102.01	12.72	77.75	8.4

10 mm/year for a core depth of 5.45 m. This is very well known from many arid zones, where evaporation drops to less than 10% of the actual evaporation at water level depth of more than 2m below the land surface.

The chloride balance model applied to the same core gives an average value of 3 mm/year for the recharge rate and an infiltration coefficient ranging around 2~3 %. Time required to accumulate the chloride observed in the profile is estimated to be 77.8 years, highlighting low recharge processes.

Since conclusions are based on only one core site, results can not be extrapolated to estimate the balance of the shallow aquifer. However, the data discussed here show that isotopic and chloride data can contribute to improving the assessment of hydrological processes in arid zones.

ACKNOWLEDGMENT

This paper was reviewed by Professor Cheikh Becaye Gaye from the University Cheikh Anta Diop of Dakar, Senegal; and by Professor Klaus-Peter Seiler from the GSF-Institute of Hydrology, Neuherberg, Germany.

REFERENCES

Allison, G.B. and M.W. Hughes. 1983. The use of natural tracers as indicators of soil-water movement in a temperature semi-arid region. *Journal of Hydrology*, vol. 60, pp. 157-173.

- Allison, G.B., C.J. Barnes, and M.W. Hughes. 1983. The distribution of deuterium and oxygen-18 in dry soils-2. Experimental. *Journal of Hydrology*, vol. 64, pp. 377-397.
- Barnes, C.J. and G.B. Allison. 1983. The distribution of deuterium and oxygen-18 in dry soils-1. Theory. *Journal of Hydrology*, vol. 60, pp. 141-156.
- Cappa, C.D., M.B. Hendricks, D.J. DePaolo, and R.C. Cohen. 2003. Isotopic fractionation of water during evaporation. *Journal of Geophysics Research*, vol. 108, 4525.
- Cook, P.G., W.M. Edmunds, and C.B. Gaye. 1992. Estimating paleorecharge and paleoclimate from unsaturated zone profiles. *Water Resources Research*, vol. 28, pp. 2721-2731.
- CRDA. 2000. Compte-rendus de fin des travaux des forages. Arrondissement des Ressources en Eaux de Gafsa, Min. de l'Agriculture et des Ressources Hydrauliques [in French]
- De Vries, D.A., and A.J. Kruger. 1967. On the value of the diffusion coefficient of water vapor in air. In: *Phénomènes des transports avec changements de phases dans les milieux poreux ou colloïdes*, pp. 61-72. Colloques internationaux, CNRS Symposium, Paris.
- Doering, E.J., R.C. Reeve, and K.R. Stockinger. 1963. Salt accumulation and salt distribution as an indicator of evaporation from fallow soils. *Soil Sciences*, vol. 97, pp. 312-319.
- Edmunds, W.M., and N.R.G. Walton. 1980. A Geochemical and Isotopic Approach to recharge Evaluation in Semi-Arid Zones: Past and Present. *Proceeding of a Symposium on Arid Zone Hydrology Investigations with Isotope Techniques*. IAEA, Vienna.
- Edmunds, W.M., E. Fellman, and I. Goni. 1999. Lakes, groundwater and palaeohydrology in the Sahel of NE Nigeria: evidence from hydrogeochemistry. *Journal of Geological Society*, vol. 156, pp. 345-355.
- Farhat, H., and L. Moumni. 1989. Etude hydrogéologique du bassin de Gafsa-nord. Direction Générale des Ressources en Eau. Min. de l'Agriculture et des Ressources Hydrauliques [in French]
- Fontes, J.Ch., M. Yousfi, and G.B. Allison. 1986. Estimation of long term, diffuse groundwater discharge in the northern Sahara using stable isotope profiles in soil water. *Journal of Hydrology*, vol. 86, pp. 315-327.
- Gaye, C.B., and W.M. Edmunds. 1996. Groundwater recharge estimation using chloride, stable isotopes and tritium profile in the sands of northwestern Senegal. *Environmental Geology*, vol. 27, pp. 246-251.
- Gouvea Da Silva Rosa, B. 1980. Migration des sels et des isotopes lourds à travers des colonnes de sédiment non saturé sous climat semi-aride. Thèse 3^{ème} cycle Sciences, Paris-Sud [in French].
- Grünberger, O. 1989. Etude géochimique et isotopique de l'infiltration sous climat tropical contrasté – Massif du Piton des neiges - Ile de la Réunion. Thèse Université de Paris-Sud [in French].
- IAEA/WMO. 2004. Global Network of Isotopes in Precipitation. The GNIP Database. Accessible at: <http://isohis.iaea.org>
- IGIP. 1998. Bassin hydraulique de Gafsa Nord. Hydrogéologie. Projet d'assistance technique aux AIC des oasis de Gafsa. Mars 1998. C.R.D.A. Gafsa [in French]
- Liu, B., F. Phillips, H. Hoiner, A.R. Campbell, and P. Sharma. 1995. Water movement in desert soil traced by oxygen isotopes, chloride, chlorine-36, southern Arizona. *Journal of Hydrology*, vol. 168, pp. 91-110.
- Merlivat, L. 1978. The dependence of bulk evaporation coefficients on air-water interfacial conditions as determined by isotopic method. *Journal of Geophysics Research*, vol. 83(C6), pp. 2977-2980.
- Musy, A. and M. Soutter. 1991. *Physique du sol*. Ed. Presses Polytechniques et Universitaire Romandes, Collection « Gérer l'Environnement » [in French].
- Penman, H.L. 1940. Gas and vapor movement in soil. *Int. Agriculture Sciences* 30: 437-462.
- Scanlon, B.R. 1991. Evaluation of moisture flux from chloride data in desert soils. *Journal of Hydrology*, vol. 128, pp. 137-156.
- Sonntag, C., D. Christmann, and K.O. Münnich. 1985. Laboratory and field experiments on infiltration and evaporation of soil water by means of deuterium and oxygen-18. IAEA-TECDOD, vol. 357, pp. 145-159.
- Taupin, J.D. 1995. Comparison of isotopic (¹⁸O and ²H) and chemical (Cl⁻) methods to calculate the dry season evaporation rate of near surface groundwater in a sahelian region – Niamey (Niger). In: *Application of tracers in arid zone hydrology (Proceeding of the Vienna Symposium)*, IAHS Publication, vol.232, pp. 339-350.

- Yermani, M. 2000. Contribution à l'étude du fonctionnement hydrodynamique du système aquifère de Gafsa Nord (Tunisie Centrale) - Apport de l'hydrochimie et de la géochimie isotopique. Thèse Doctorat, Université de Tunis-el Manar [in French].
- Zimmermann, U., D. Ehhalt, and K.O. Münnich. 1966. Soil water movement and evapotranspiration: Changes in the isotopic composition of water. In: Isotopes Hydrology, Proceeding of IAEA Symposium, pp. 567-585.

ADDRESS FOR CORRESPONDENCE

Messaouda Yermani
Departement de Biologie-Géologie
Institut Préparatoire aux Etudes d'Ingénieurs de Bizerte
Zarzouna 7021
Tunisia

Email: yermanim@yahoo.fr
